Electrostatic Analysis of a Short Accident in Cable Trays for Intelligent Pressure Transmitters

Jaeyul Choo, Sang Yong Jeong, Hyung Tae Kim, Yeong Jin Yu, Hyun Shin Park, and Choong Heui Jeong

Korea Institute of Nuclear Safety, 62 Gwahak-ro, Yuseong-gu, Daejeon, Korea
k728cjy@kins.re.kr, k728jsy@kins.rer.kr, k719kht@kins.re.kr, k644yyj@kins.re.kr, k394phs@kins.re.kr, chjeong@kins.re.kr

Abstract

We apply the mode-matching method to the electrostatic analysis of shorted enclosed-cable trays that are generally used in industrial facilities such as nuclear power plants. In mode-matching formulation on the potential distribution, we utilize Laplace's equation and superposition principle. After obtaining modal coefficients from Dirichlet and Neumann boundary conditions, we then derive the potential and electric field distributions and the capacitance matrices to evaluate the electromagnetic influence due to a short accident.

1. Introduction

The cable trays have been employed to protect and isolate the power and communication cables from physical and electromagnetic damage and fire attacks in industrial facilities such as a nuclear power plant [1], [2]. Based on the configuration, the cable trays are divided into ladder-type, perforated-type, and solid-bottom-type, etc. To improve the isolation and protection performances, either the enclosed cable tray or the physical and electromagnetic barrier can be utilized [1], [2].

In this paper, we analyze the electromagnetic influence from the shorted enclosed-cable trays used for intelligent pressure transmitters in nuclear power plants. We assume that two enclosed-cable trays without connection to the ground are located between both lateral walls and shorted by the inner leaky cables. To derive the potential and electric field distributions and the capacitance matrices in the variation of geometrical parameters, we utilize the mode-matching method [3]. Since the wavelength in the operating frequency of the used power cables is generally large (about 5000 km in the operating frequency of 60 Hz) in comparison with the dimension of the analyzed regions, the electrostatic analysis can be valid in our approach. Among the investigated results, the resulted capacitance matrix generally indicates how much the enclosed-cable trays is influenced from adjacent another tray and lateral walls in a short accident. Note that the novelty of this research is the estimation of the electromagnetic influence from the shorted enclosed-cable trays. In what follows, we show a brief mode-matching formulation on the potential distribution and boundary conditions for simultaneous equations

2. Mode-matching formulation

Fig. 1 illustrates the cross section of two enclosed-cable trays with $w_1 \times h$ m^2 and $w_2 \times h$ m^2 that are long along the y–axis. The enclosed-cable trays are separated from each other with the distance s and apart from the lateral walls with the distances d_1 and d_2, respectively. As shown at the bottom of Fig. 1, due to the short by the inner leaky cables, the potentials V_1 and V_2 are applied to both enclosed-cable trays, respectively. The analyzed regions around the enclosed-cable trays are specifically composed of 5 different regions (Regions I to V). Based on the superposition principle, it is tractable that the original problem is considered the decomposed three problems in Fig. 2 where the

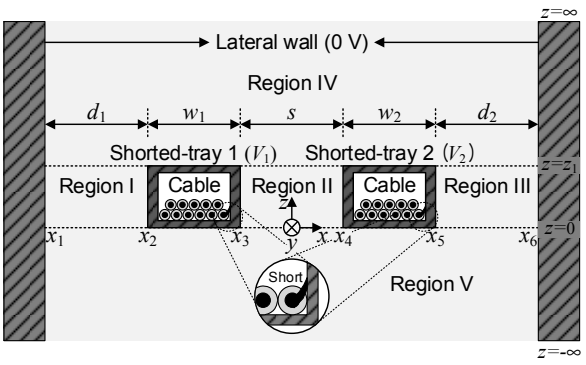

Fig. 1. Cross section of the shorted enclosed-cable trays.

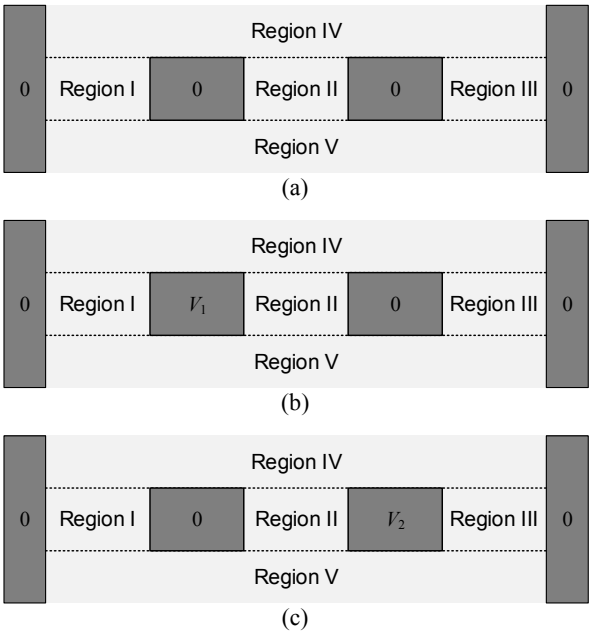

Fig. 2. Equivalent problem based on the superposition principle: (a) case 1, (b) case 2, and (c) case 3.

potentials on the enclosed-cable trays have (0, 0) in case 1, (V_1, 0) in case 2, and (0, V_2) in case 3, respectively. In addition, each case in Fig. 2 satisfies Laplace's equation as

$$\nabla^2\Phi(x,z)=0\,. \tag{1}$$

Thus, the superposition principle and the Laplace's equation yield the potential expression in each region as

$$\Phi_I(x,z)=\sum_{n_1=1}^{\infty}f_1(z)\sin m_1(x-x_1)+\frac{V_1}{d_1}(x-x_1) \tag{2}$$

$$\Phi_{II}(x,z)=\sum_{n_2=1}^{\infty}f_2(z)\sin m_2(x-x_3)+\frac{V_2-V_1}{s}(x-x_3)+V_1 \tag{3}$$

$$\Phi_{III}(x,z)=\sum_{n_3=1}^{\infty}f_3(z)\sin m_3(x-x_5)-\frac{V_2}{d_2}(x-x_6) \tag{4}$$

$$\Phi_{IV}(x,z)=\sum_{n_4=1}^{\infty}f_4(z)\sin m_4(x-x_1) \tag{5}$$

$$\Phi_V(x,z)=\sum_{n_5=1}^{\infty}f_5(z)\sin m_5(x-x_1) \tag{6}$$

where the subscript of Φ indicates each region, $m_1 = n_1\pi / (x_2 - x_1)$, $m_2 = n_2\pi / (x_4 - x_3)$, $m_3 = n_3\pi / (x_6 - x_5)$, $m_4 = n_4\pi / (x_6 - x_1)$, $m_5 = n_5\pi / (x_6 - x_1)$, and

$$f_\alpha(z)=\begin{cases}A_\alpha e^{-m_\alpha z} & , \quad \text{when } \alpha=4\\ A_\alpha e^{-m_\alpha z}+B_\alpha e^{m_\alpha z} & , \quad \text{when } \alpha=1,2,\text{and } 3\,.\\ A_\alpha e^{m_\alpha z} & , \quad \text{when } \alpha=5\end{cases}$$

To determine the unknown modal coefficients A_1, A_2, A_3, A_4, A_5, B_1, B_2, and B_3, the Dirichlet conditions for the continuity of potentials and the Neumann conditions for the continuity of normal derivatives of the potentials at $z = h$ are represented as, respectively,

$$\Phi_{IV}(x,z)\big|_{z=h}=\begin{cases}\Phi_I(x,z)\big|_{z=h} & , \quad x_1\le x<x_2\\ V_1 & , \quad x_2\le x<x_3\\ \Phi_{II}(x,z)\big|_{z=h} & , \quad x_3\le x<x_4\\ V_2 & , \quad x_4\le x<x_5\\ \Phi_{III}(x,z)\big|_{z=h} & , \quad x_5\le x<x_6\end{cases} \tag{7}$$

$$\left.\frac{\partial\Phi_I(x,z)}{\partial z}\right|_{z=h}=\left.\frac{\partial\Phi_{IV}(x,z)}{\partial z}\right|_{z=h} \quad , \quad x_1\le x<x_2 \tag{8}$$

$$\left.\frac{\partial\Phi_{II}(x,z)}{\partial z}\right|_{z=h}=\left.\frac{\partial\Phi_{IV}(x,z)}{\partial z}\right|_{z=h} \quad , \quad x_3\le x<x_4 \tag{9}$$

$$\left.\frac{\partial\Phi_{III}(x,z)}{\partial z}\right|_{z=h}=\left.\frac{\partial\Phi_{IV}(x,z)}{\partial z}\right|_{z=h} \quad , \quad x_5\le x<x_6\,. \tag{10}$$

Then equations (7)–(10) for the Dirichlet and Neumann conditions respectively yield

$$\begin{aligned}&\sum_{n_1=1}^{\infty}F(x_1,x_2,m_1,p_4)f_1(h)+\sum_{n_2=1}^{\infty}F(x_3,x_4,m_2,p_4)f_2(h)\\&+\sum_{n_3=1}^{\infty}F(x_5,x_6,m_3,p_4)f_3(h)+\frac{x_1-x_6}{2}\sum_{n_4=1}^{\infty}f_4(h)\delta_{m_4p_4}\\&=-\frac{V_1}{d_1}g(x_1,x_2)+\frac{V_1-V_2}{s}g(x_3,x_4)-\frac{V_2}{d_2}g(x_6,x_5)\\&+\frac{V_1-V_2}{p_4}\cos p_4(x_1-x_4)-\frac{V_1}{p_4}\cos p_4(x_1-x_2)\\&+\frac{V_2}{p_4}\cos p_4(x_1-x_5)\end{aligned} \tag{11}$$

$$\begin{aligned}&\sum_{n_1=1}^{\infty}\frac{x_1-x_2}{2}\delta_{m_1p_1}d_1(h)\\&+\sum_{n_4=1}^{\infty}F(x_1,x_2,x_1,p_1,m_4)d_4(h)=0\end{aligned} \tag{12}$$

$$\begin{aligned}&\sum_{n_2=1}^{\infty}\frac{x_3-x_4}{2}\delta_{m_2p_2}d_2(h)\\&+\sum_{n_4=1}^{\infty}F(x_3,x_4,x_1,p_2,m_4)d_4(h)=0\end{aligned} \tag{13}$$

$$\begin{aligned}&\sum_{n_3=1}^{\infty}\frac{x_5-x_6}{2}\delta_{m_3p_3}d_3(h)\\&+\sum_{n_4=1}^{\infty}F(x_5,x_6,x_1,p_3,m_4)d_4(h)=0\end{aligned} \tag{14}$$

where

$$F(a,b,c,m,p)=\int_a^b\sin m(x-a)\sin p(x-c)dx$$

$$g(\beta,\gamma)=\int_\beta^\gamma(x-\beta)\sin p_4(x-x_1)dx$$

$$d_\alpha(\beta)=\left.\frac{df_\alpha(z)}{dz}\right|_{z=\beta}\,.$$

For the bottom regions, it is possible to enforce the boundary conditions at $z = 0$ through the similar procedure. The results from the enforcement of boundary conditions at $z = 0$ and $z = h$ constitute a set of simultaneous equations for obtaining the modal coefficients A_1, A_2, A_3, A_4, A_5, B_1, B_2, and B_3. The modal coefficients are calculated efficiently after truncating the infinite series in the simultaneous equations.

3. Computation results

The numerical computation was performed using Matlab program language. In our computation, it is important to determine the proper truncation number to ensure convergence of the potential values since the excessive series for the potentials require much computing time. After verifying the fast convergence, we derived the potential and electric field distributions and the capacitance matrices.

3.1. Potential and electric field distribution

The electric field distribution can be computed from the gradient of the potential as [3]

$$\overline{E}(x,z) = -\nabla\Phi(x,z)\,. \tag{15}$$

Figs. 3 and 4 show the electric field strength of x−component (Ex) and z−component (Ez) for the shorted enclosed-trays with the applied potentials of $V_1 = -1$ and $V_2 = 1$ where the geometry parameters are $w_1 = s = w_2 = 5$ m and $d_1 = d_2 = 10$ m. The electric fields are normalized by the absolute potential difference $|V_2 - V_1|$ between two enclosed-trays. Due to the symmetry with respect to y–z plane, both results in Figs. 3 and 4 are seen to be symmetrical distributions.

In Fig. 3, the equivalent potential lines are dense between two enclosed-trays (in Region II), which results in strong electric field and electromagnetic coupling. In addition, the equivalent potential lines are tilted to the direction of the lateral walls that indicates the distance d_1 and d_2 are also the important factors influencing on the nearby enclosed-cable trays electromagnetically. Fig. 4 shows the investigation of the electric field strength calculated by (15). As expected, Ex is forceful at the gap between both enclosed-trays (Region II) and in the space between the enclosed-trays and the lateral walls (Regions I and III). These investigated results would be able to provide proper geometry about the distances d_1, s, and d_2 to avoid the unwanted electromagnetic interference (EMI) problems.

3.2. Capacitance matrix

Computation was performed to examine the capacitance matrix because it also indicates the electrostatic influence on adjacent objects. The capacitance matrix C is defined as [4]

$$[C] = \begin{bmatrix} C_{11} & -C_{12} \\ -C_{21} & C_{22} \end{bmatrix} \tag{16}$$

where each component for the symmetric structure is obtained as

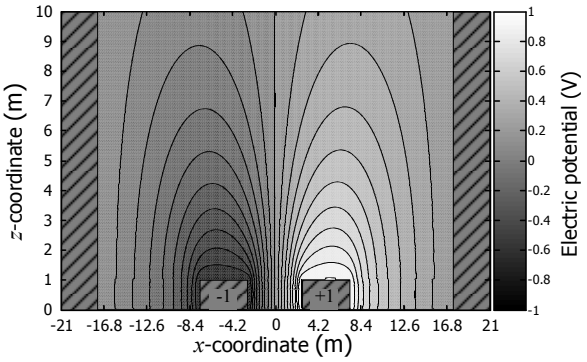

Fig. 3. Potential distribution ($w_1 = s = w_2 = 5$ m, $d_1 = d_2 = 10$ m, $V_1 = -1$, and $V_2 = 1$).

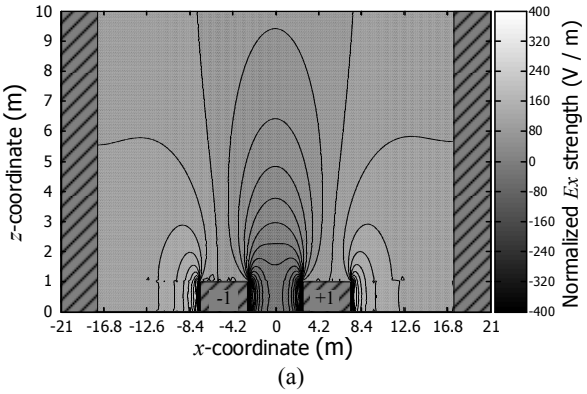

(a)

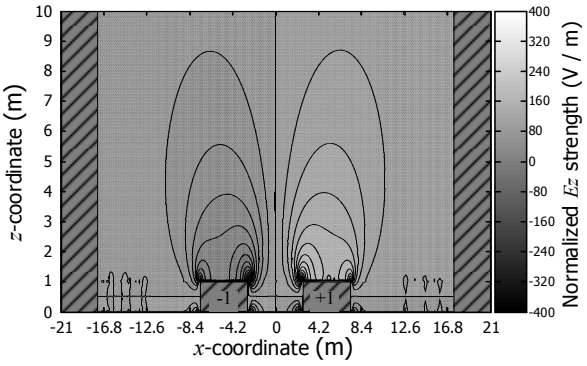

(b)

Fig. 4. Distribution of electric field strength: (a) x–component (E_x) and (b) z–component (E_z) of electric field strength ($w_1 = s = w_2 = 5$ m, $d_1 = d_2 = 10$ m, $V_1 = -1$, and $V_2 = 1$).

$$C_{11} = C_{22} = \left.\frac{Q_1}{V_1}\right|_{V_2=0} = \left.\frac{Q_2}{V_2}\right|_{V_1=0}$$

$$C_{11} = C_{22} = \left.\frac{Q_1}{V_1}\right|_{V_2=0} = \left.\frac{Q_2}{V_2}\right|_{V_1=0}\,.$$

Herein both Q_1 and Q_2 represent the charge accumulation per unit length (m) on the shorted enclosed-cable trays 1 and 2,

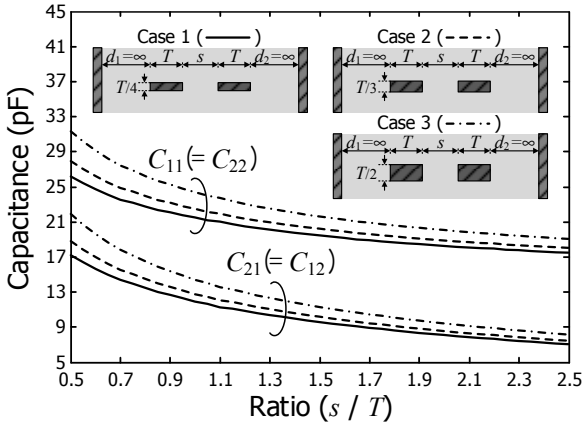

Fig. 5. Capacitances C_{11} and C_{21} of both shorted enclosed-cable trays with horizontally parallel placement when the separation distance s varies (case 1: $w_1 = w_2 = T$ and $h = T$ / 4, case 2: $w_1 = w_2 = T$ and $h = T$ / 3, and case 3: $w_1 = w_2 = T$ and $h = T$ / 2).

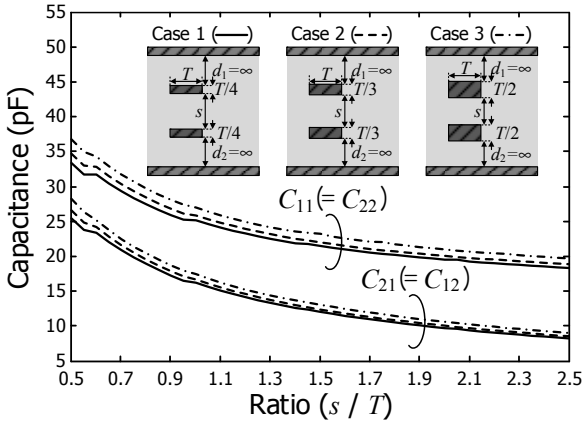

Fig. 6. Capacitances C_{11} and C_{21} of both shorted enclosed-cable trays with vertically parallel placement when the separation distance s varies (case 1: $w_1 = w_2 = T$ / 4 and $h = T$, case 2: $w_1 = w_2 = T$ / 3 and $h = T$, and case 3: $w_1 = w_2 = T$ / 2 and $h = T$).

respectively, and are calculated using the integral form of Gauss's law as

$$\oint_{Tray\,1,2} \bar{D} \cdot d\bar{l} = \varepsilon_0 \oint_{Tray\,1,2} \bar{E} \cdot d\bar{l} = Q_{1,2} \qquad (17)$$

Figs. 5 and 6 show the capacitance matrices when both shorted enclosed-cable trays are close to each other horizontally and vertically, respectively. To reveal electrostatic influence only between both shorted cable trays excluding that from the lateral walls, the distances d_1 and d_2 were set the infinite distance (over 10 times distance of $2T + s$). In Figs. 5 and 6, the capacitances C_{11} and C_{21} are shown to be enlarged when the height of the cable trays increases from T / 4 (case 1) to T / 2 (case 3) as well as the ratio s / T decreases. The investigated results reveal that the separation distance s should be significantly considered in the place with the accumulated the cable trays in order to avoid the EMI problems.

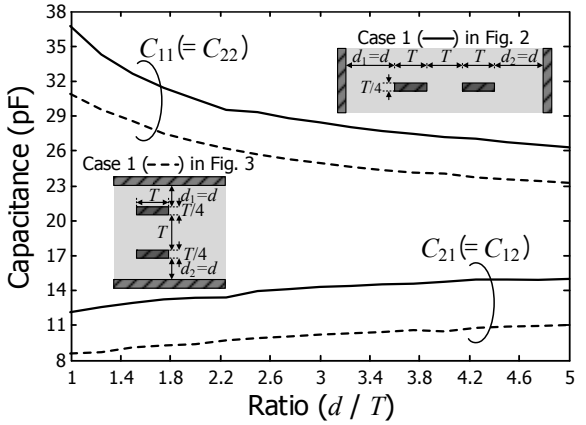

Fig. 7. Capacitances C_{11} and C_{21} of the cases 1 in Figs. 2 and 3 when the distance d ($= d_1 = d_2$) changes and the separation distance s is T.

In Fig. 7, we investigated the capacitance C_{11} and C_{21} corresponding to variation in the distance d ($= d_1 = d_2$) in cases 1 in Figs. 5 and 6 for evaluating the effect from the lateral walls. In both cases 1, the capacitance C_{11} is shown to be increased whereas the capacitance C_{21} is shown to be decreased when the lateral walls approach to the shorted enclosed-cable trays. The deviation between the capacitances C_{11} and C_{21} gives a clue about the favorable placement of the grounded structure to alleviate the undesirable electromagnetic coupling from nearby objects.

4. Conclusions

The mode-matching method was applied to the electrostatic analysis of the shorted enclosed-cable trays for the intelligent pressure transmitter in nuclear power plants. The mathematical expressions with the unknown modal coefficients for potential distribution were formulated based on Laplace's equation and superposition principle. The modal coefficients with the proper truncation number were then determined from the Dirichlet and Neumann boundary conditions. Using the obtained modal coefficients, we investigated the potential and electric field distributions and the capacitance matrices corresponding to the change in placement of the shorted cable trays and the lateral walls. The investigated results offer the useful information to avoid EMI problems in nuclear power plants.

5. Acknowledgment

This work was supported by the Korea Institute of Nuclear Safety under the project 'Development of Proof Test Model and Safety Evaluation Techniques for the Regulation of Digital I&C Systems used in NPPs' (no. 1305003–0315–SB130).

6. References

[1] M. J. A. M. v. Helvoort, "Grounding structures for the EMC-protection of cabling and wiring", Eindhoven University Eindhoven, Eindhoven, Netherland, 1995.

[2] *IEEE Standard Criteria for Independence of Class 1E Equipment and Circuits*, IEEE Standard 384, 2008.

[3] H. J. Eom, "Electromagnetic Wave Theory for Boundary-value Problems", Springer Verlag, Berlin, Germany, 2004.

[4] C. Wei, R. F. Harrington, J. R. Mautz, and T. K, Sarkar, "Multiconductor transmission lines in multilayered dielectric media," *IEEE Trans. Microw. Theory Tech*., vol. 32, no. 4, pp. 439–450, Apr., 1984.